

Effects of low attenuation in a nanomechanical electron shuttle

Dominik V. Scheible^{a)}

Center for NanoScience and Fakultät für Physik der Ludwig-Maximilians-Universität,
Geschwister-Scholl-Platz 1, 80539 München, Germany

Christoph Weiss

Institut für Physik, Carl-von-Ossietzky-Universität, 26111 Oldenburg, Germany

Robert H. Blick

Electrical & Computer Engineering, University of Wisconsin-Madison, 1415 Engineering Drive,
Madison, Wisconsin 53706

(Received 3 March 2004; accepted 11 May 2004)

We have measured the spectral current characteristics of a nanomechanical electron shuttle in a tuning-fork configuration. This particular design enhances the quality factor Q of the nanoelectromechanical system. Comparing the experimental results to a precedingly studied low- Q device, we find a substantially different current behavior, indicating an increase of Q : the current flips direction around the frequency of mechanical resonance. We support our conclusion with a model calculation via a master equation. The device is nanomachined in silicon and shows response up to 0.5 GHz at room temperature. © 2004 American Institute of Physics.
[DOI: 10.1063/1.1767966]

Mechanical clocking of charge transfer can be achieved on a macroscopic scale by the placing of a suspended metallized particle between the two plates of a condenser.¹ Such a setup operates typically in the audible frequency range of 100 Hz–1 kHz. With the advent of nanoelectromechanical systems (NEMS) (Ref. 2) it is now possible to realize mechanical devices reaching fundamental eigenfrequencies above 1 GHz.³ The straightforward application of NEMS as an electron shuttle allows to clock electron tunneling at radio frequencies in a pendulum setup, machined in silicon.⁴ Realization of the concept in this material paves the way for application of such NEMS electron shuttles as low power-loss filters in communication technology.⁵ Furthermore, the interplay of mechanical and electronic systems at the nanometer scale may grant access to quantum-limited detection of forces and displacements.⁶

However, the major drawback of NEMS—usually processed in classical semiconductor crystals, such as silicon or gallium arsenide—is the dramatically reduced mechanical quality factor Q : compared to macroscopic mechanical resonators this reduction is as large as four to five orders of magnitude.⁷ The physical mechanism responsible for this reduction is still subject to scientific debate,⁸ although it appears today that dislocations in the coating top metal layer of NEMS are the main cause of this limitation.⁹ Manufacturing NEMS in other material systems than silicon, such as diamond, yields a maximum of $Q \sim 10^4$.¹⁰ An alternative approach, achieving comparable results, is the optimization of the resonator geometry in order to minimize the dissipation of the oscillation energy, as in a tuning fork.¹¹ We have shown an enhancement of the quality factor of such a tuning-fork NEMS in earlier works.^{12,13} Here, we apply and model

this concept to a nanomechanical electron shuttle whose dynamic response is usually probed by the transported net current.⁴

The layout of the device comprises several generations of electron shuttle designs and detailed engineering of its mechanical properties.^{4,12–14} Figure 1(a) shows the NEMS, consisting of a doubly clamped and fully metallized central beam resonator, with two identical cantilevers on either side. The latter couple mechanically to the central beam, forming a tuning fork with minimum dissipation within the structure. Metallization reaches approximately half a micron up to the single electron islands on the outer left and right, which are supported by insulating silicon beams. The device was fabricated from silicon-on-insulator material, employing elec-

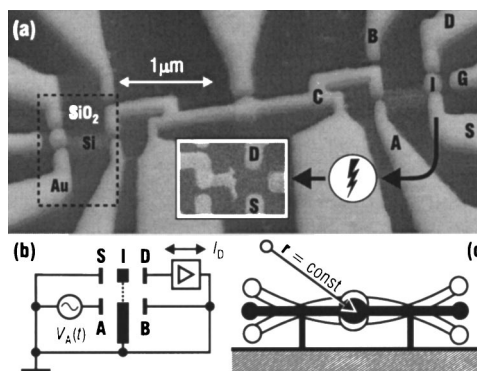


FIG. 1. (a) Scanning electron beam micrograph of the device, consisting of a doubly clamped central beam and two shuttle clappers at either side. At their end we have deposited the metallic islands I, which are of the dimensions $80 \times 80 \times 50 \text{ nm}^3$. The right hand shuttle is seen with gate labels A through S. The inset shows the blown island, after application of a destructive voltage pulse. (b) The equivalent circuit of the experimental setup: a signal generator provides the ac voltage $V_A(t)$ at an incident power P and at frequency f . (c) Schematic of a linear tuning fork. During oscillation the center of mass $\mathbf{r}(t) = \text{const}$ remains fixed in space, and therefore reduces energy dissipation into the suspension.

^{a)}Author to whom correspondence should be addressed; electronic mail: dominik.scheible@lmu.de

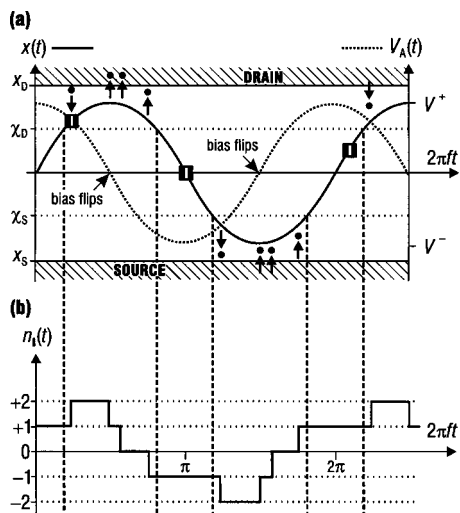


FIG. 2. (a) Shuttle deflection $x(t)$ and gate voltage $V_A(t)$ with a relative phase of $\phi = -\pi/2$. The arrows indicate electron flux from or to the island I, which results in a positive net source-drain current I_D in this particular case. (b) Charge state of the island $n_i(t)$ over time. Tunneling is suppressed when the shuttle is inside $[\chi_S, \chi_D]$.

tron beam lithography and anisotropic reactive ion etching. This so-called sacrificial layer process we have demonstrated elsewhere.¹² The device is mounted in a probe station that allows measurement from dc up to several GHz, as well as operation from room temperature down to 77 K. Gate A is connected to a synthesizer that provides the ac signal at frequency f and at incident power P . The current is detected at drain D by a current amplifier [see equivalent circuit in Fig. 1(b)].

As in preceding works,^{4,15} we employ the theoretical tool of a master equation^{16,17} to model the current transport across the island with the mechanical degree of freedom: a differential equation relates the time-dependent probability $p(n, t)$ to find n additional electrons on the island to the transition rates $\Gamma_i^\pm(n, t)$ at either barrier ($i = S, D$). In the pure tunneling regime these rates can be derived from Fermi's golden rule. In the present case of a periodic motion and a time-dependent gate voltage $V_A(t)$, the rates are thus of the form:

$$\Gamma_i^\pm(n, t) = \frac{1}{\tau_i(t)} \frac{\mp [n + C_A(t)V_A(t)/e] - 1/2}{1 - \exp\{\pm \vartheta [n + C_A(t)V_A(t)/e - 1/2]\}}, \quad (1)$$

where $\tau_i(t)$ are the RC-time constants of the tunneling between island and electrode i , and $\vartheta = [C_S(t) + C_D(t) + C_A(t)]k_B T/e^2$. The C_j are the respective capacitances between the island I and gate j . Since the resistance, and therefore the tunneling rates, depend exponentially on the shuttle deflection, tunneling is only possible when the island is close to one of the electrodes' source or drain.^{4,16} Thus, we define characteristic shuttle displacements toward source and drain, χ_S and χ_D , respectively, in the way that tunneling is negligible for a shuttle displacement $x(t)$ inside the interval $[\chi_S, \chi_D]$.

An ac gate voltage $V_A(t) \propto \sin(2\pi ft)$ leads to a periodic force exerted onto the island. In principle, this force is a superposition of a capacitive force $\propto V_A^2$ and the Coulomb

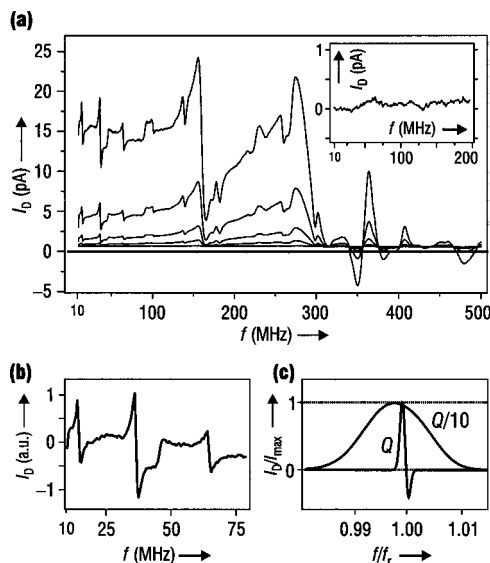


FIG. 3. (a) Experimental current traces I_D vs frequency f for a set of incident ac powers $P = -30$ to -10 dBm. The inset shows the current breakdown after the island has blown. (b) Magnification of the particular current behavior around a mode resonance: the current flips sign (superimposed onto a thermal background of the rest of the spectral response). (c) Calculated transported net current via a master equation. Enhancing the quality factor Q by a factor of 10 reveals a current flip.

force on the charged island. In a simple two-terminal setup we have recently confined the excitation to the Coulomb force onto the excess charge.¹⁸

We can model the equation of motion of the shuttle via a periodically driven damped harmonic oscillator, with its solution¹⁹

$$x(t) = \bar{x}(f) \sin[2\pi ft + \phi(f)], \quad (2)$$

and the phase shift

$$\phi(f) = \tan^{-1}\left(\frac{kf}{f_0^2 - f^2}\right). \quad (3)$$

As usual, for low frequencies the force and the motion are in phase whereas for high frequencies the motion is in opposite phase. In the experiment, we detect only a current close to the resonance frequency (for other frequencies the current is exponentially suppressed). In the case of a weakly damped pendulum, the frequency for which the motion is changing from in phase to opposite phase is close to the resonance frequency. We will see that this leads to a particular spectral current behavior, which is not visible for a strongly damped shuttle.

The phase shift of Eq. (3) relates the pendulum's motion to the local ac electric field, which determines the spectral current behavior of the device, i.e., the amount and direction of charge transported by the shuttle for an applied excitation frequency f . In Fig. 2(a) we have drawn the shuttle deflection $x(t)$ and the gate voltage $V_A(t)$ with a phase shift of $\phi = -\pi/2$. As can be retraced from Fig. 2, net current flows from source to drain in this case, since more electrons tunnel from source onto the shuttle and from the shuttle to drain than vice versa.

In Fig. 3(a) we show the spectral current traces in their

averaged form for a set of varying incident powers P . The maximum power corresponds to a voltage amplitude of $\bar{V}_A \approx 70$ mV. The phase relation $\phi_h(f)$ for each mode h changes during the frequency sweep, according to Eq. (3). The resultant spectral current $I_D(f)$ is a superposition of all inherent modes of the cantilever and a thermally supported current toward lower frequencies ($f \lesssim 300$ MHz). At liquid nitrogen temperature this background vanishes.¹⁵ In Fig. 3(b) we have magnified a set of resonances, revealing the phase dependence of the current and resulting in the reversal of its direction. This was not observed for a low- Q variant of the shuttle with an experimentally determined $Q \sim 10$.⁴ In the model calculation, the current flip is reproduced by increasing the mechanical quality Q by a factor of 10, holding all remaining parameters constant. A precise calculation of Q from the data requires values of the characteristic shuttle deflections χ_i , which are not accessible in the present experimental setup, and is therefore difficult. Nevertheless, both the qualitative behavior and the model calculations show that the Q factor is increased; from preceding experiments,¹³ we estimate the mechanical quality factor Q of the cantilever to be in the range $10^2 - 10^3$.

The final stage of experiments on this nanomechanical resonator was the application of destructive voltage pulses. This served the purpose of a control experiment, and proved the mechanical origin of the current. At a sufficiently high dc bias, $V_S \sim 10$ V at source S, the tiny island blew like a fuse [cf. Fig. 1(a)] and the current signal broke down, as shown in the inset of Fig. 3(a).

In conclusion, we have applied the concept of a linear tuning fork to a nanomechanical electron shuttle. Comparison of the attained spectral current characteristics to the data of a shuttle in a simple clapper design, in concert with a

model calculation, points to a substantially reduced dissipation in this device.

Authors would like to thank J. P. Kotthaus for his continuous support and F. W. Beil for stimulating discussions. D.V.S. gratefully acknowledges financial support by the Deutsche Forschungsgemeinschaft (DFG) under Grant No. BI-487.

¹P. Benjamin, *The Intellectual Rise in Electricity* (Appleton, New York, 1895).

²R. H. Blick *et al.*, J. Phys.: Condens. Matter **14**, R905 (2002).

³X. M. H. Huang, C. A. Zorman, M. Mehregany, and M. L. Roukes, Nature (London) **421**, 496 (2003).

⁴A. Erbe, C. Weiss, W. Zwerger, and R. H. Blick, Phys. Rev. Lett. **87**, 096106 (2001).

⁵C. T.-C. Nguyen, IEEE Trans. Microwave Theory Tech. **47**, 1486 (1999).

⁶M. L. Roukes, Phys. World **14**, 25 (2001).

⁷W. Duffy, J. Appl. Phys. **68**, 5601 (1990).

⁸R. Lifshitz and M. L. Roukes, Phys. Rev. B **61**, 5600 (2000).

⁹F. W. Beil, R. H. Blick, A. Wixforth, W. Wegscheider, M. Bichler, and D. Schuh (unpublished).

¹⁰A. B. Hutchinson, P. Truitt, K. C. Schwab, L. Sekaric, J. M. Parpia, H. G. Craighead, and J. E. Butler, Appl. Phys. Lett. **84**, 972 (2004).

¹¹W.-T. Hsu, J. R. Clark, and C. T.-C. Nguyen, Technical Digest International Conference on Solid State Sensors & Actuators, 1110 (2001).

¹²D. V. Scheible, A. Erbe, and R. H. Blick, New J. Phys. **4**, 86.1 (2002).

¹³D. V. Scheible, A. Erbe, and R. H. Blick, Appl. Phys. Lett. **82**, 3333 (2003).

¹⁴SOLVIA finite element solver, version 99.0.

¹⁵D. V. Scheible, C. Weiss, J. P. Kotthaus, and R. H. Blick (unpublished).

¹⁶C. Weiss and W. Zwerger, Europhys. Lett. **47**, 97 (1999).

¹⁷L. Y. Gorelik, A. Isacsson, M. V. Voinova, B. Kasemo, R. I. Shekhter, and M. Jonson, Phys. Rev. Lett. **80**, 4526 (1998).

¹⁸D. V. Scheible and R. H. Blick, Appl. Phys. Lett. **84**, 4632 (2004).

¹⁹The deflection amplitude of the driven harmonic oscillator is

$$\bar{x}(f) \propto 1/\sqrt{(f^2 - f_r^2)^2 + \gamma^2 f^2}$$

with the dynamic attenuation $\gamma \propto Q^{-1}$ and the shifted frequency of the damped oscillator

$$f_r = f_0 \sqrt{1 - 1/(2Q^2)}.$$